A new modulated structure in α-Fe_2O_3 nanowires*

Cai Rong-Sheng(蔡鎔声)[a], Shang Lei(商 蕾)[a], Liu Xue-Hua(刘雪华)[a,b], Wang Yi-Qian(王乙潜)[a,†], Yuan Lu(袁 露)[c], and Zhou Guang-Wen(周光文)[c]

[a] *The Cultivation Base for State Key Laboratory, Qingdao University, Qingdao* 266071, *China*

[b] *Laboratory of Advanced Materials and Electron Microscopy, Institute of Physics, Chinese Academy of Sciences, Beijing* 100190, *China*

[c] *Department of Mechanical Engineering & Multidisciplinary Program in Materials Science and Engineering, State University of New York, Binghamton, NY* 13902, *USA*

(Received 18 March 2013; revised manuscript received 27 April 2013)

A new modulated structure consisting of periodic $(11\bar{2}0)$ stacking faults (SFs) in the α-Fe_2O_3 nanowires (NWs) formed by the thermal oxidation of Fe foils is reported, using a combination of high-resolution transmission electron microscopy (HRTEM) observations and HRTEM image simulations. The periodicity of the modulated structure is 1.53 nm, which is ten times $(3\bar{3}00)$ interplanar spacing and can be described by a shift of every ten $(3\bar{3}00)$ planes with 1/2 the interplanar spacing of the $(11\bar{2}0)$ plane. An atomic model for the Fe_2O_3 structure is proposed to simulate the modulated structure. HRTEM simulation results confirm that the modulated structure in α-Fe_2O_3 NWs is caused by SFs.

Keywords: crystal structure, nanocrystalline materials, electron microscopy, simulation and modeling

PACS: 74.62.Bf, 75.50.Tt, 87.64.Ee, 61.43.Bn **DOI:** 10.1088/1674-1056/22/10/107401

1. Introduction

Hematite (α-Fe_2O_3) has received much attention because of its chemical stability in ambient conditions,[1,2] low toxicity, and great potential for a wide range of applications in gas sensors, electrode materials,[3] magnetic recording media,[4] pigments,[5] and spintronic devices.[6] It is an n-type semiconductor with a band gap of 2.1 eV. Recently, α-Fe_2O_3 nanowires (NWs) have been successfully fabricated by the thermal oxidation of iron (Fe) in an oxygen-containing atmosphere.[5,7–13] Extensive studies have been carried out to understand the growth mechanism of these NWs.[14–16] However, detailed microstructural information is also needed to develop a better understanding of the growth processes. In our earlier study of Fe_2O_3 NWs,[17] the growth mechanism was discussed, but the modulated structure was not investigated comprehensively. Modulated structures play an important role in the synthesis, stabilization and properties of many systems such as InAs/InP[18] and n-Si/p-Si[19] NWs. Naturally occurring modulated structures have been demonstrated in ZnS[20] and ZnSe[21] NWs. Therefore, it is significant to clarify the microstructure of the modulated structures since it could provide significant insights into how to control the microstructure of the NWs and, correspondingly, their properties for practical applications.

In this paper, we report our investigation of the microstructure of a modulated structure in Fe_2O_3 NWs synthesized by the thermal oxidation of Fe using HRTEM. It is found that the modulated structure is formed by stacking faults (SFs). Based on our HRTEM observations, a new atomic model is proposed to explain this modulated structure, which is further confirmed by HRTEM image simulations. In addition, electron energy-loss spectroscopy (EELS) has been carried out to confirm the existence of SFs in the NWs.

2. Experiment

The Fe_2O_3 NWs were synthesized by the thermal oxidation of Fe foils. First, the high-purity (99.99%) Fe foils were rinsed with deionized water followed by ultrasonication in acetone for 5 min. Then the cleaned Fe substrates were put on a substrate heater in a vacuum chamber, and the temperature was monitored using a K-type thermocouple in contact with the heater. The chamber was pumped to a vacuum of about 2×10^{-6} Torr, and then filled with 200-Torr-oxygen (oxygen purity: 99.999%) (1 Torr$= 1.33322 \times 10^2$ Pa). Subsequently, the chamber was sealed and the Fe foil was heated to 600 °C at a rate of 20 °C/min in the oxygen gas. After the Fe foil was oxidized for 1 h, it was cooled down in the same oxygen atmosphere to room temperature at a rate of ~ 10 °C/min.

Transmission electron microscope (TEM) samples of Fe_2O_3 NWs were prepared by peeling off the black product from the surface of the oxidized Fe foil, ultrasonicating them in ethanol for several minutes, and dispersing a drop onto a holey-carbon-film-coated copper grid. Selected-area electron diffraction (SAED), bright field (BF), and HRTEM examina-

*Project supported by the National Key Basic Research Development Program of China (Grant No. 2012CB722705), the Natural Science Foundation for Outstanding Young Scientists in Shandong Province, China (Grant No. JQ201002), the Program for Foreign Cultural and Educational Experts (Grant No. 20123702083), the Program for Higher Education Science and Technology in Shandong Province (Grant No. J12LA17). Wang Yi-Qian would like to thank the financial support from Taishan Outstanding Overseas Scholar Program of Shandong Province, China.

†Corresponding author. E-mail: yqwang@qdu.edu.cn

tions were carried out using a JEOL JEM 2100F TEM operating at 200 kV. EELS was performed on an FEI Tecnai F20 TEM. The EELS spectra were acquired in an image mode with a collection half angle of ∼16 mrad.

3. Results and discussion

After the thermal oxidation of Fe foils in oxygen atmosphere, three different kinds of NWs are relatively aligned and perpendicular to the substrate surface, namely, single-crystalline, bi-crystalline and tri-crystalline NWs. The growth mechanism of the Fe_2O_3 NWs was investigated in our previous work.[17] Herein, we focus on developing a detailed understanding of the microstructure of the single-crystalline Fe_2O_3 NWs, since far fewer reports have been published on this structure than on the other structures. By examining many individual single-crystalline NWs, we identify a previously unobserved modulated structure in these NWs. Figure 1(a) shows a typical bright-field (BF) TEM image of an Fe_2O_3 NW with a diameter of about 25 nm. The NW has a smooth surface. Figure 1(b) is a typical SAED pattern of the NW in Fig. 1(a), which corresponds to a [0001] zone-axis of hexagonal α-Fe_2O_3. The growth direction for the NW can be determined to be $[11\bar{2}0]$. It can be found that superlattice diffraction spots exist in the SAED pattern, which are indicated by arrows. HRTEM images were taken to clarify the origin of these superlattice diffraction spots. Figure 1(c) shows a [0001] zone-axis HRTEM image obtained from the NW in panel (a). This HRTEM image is taken with a defocus value of about 58 nm. In Fig. 1(c), $(3\bar{3}00)$ lattice planes are marked by two parallel white lines. To further clarify the nature of the structural modulation, an enlarged HRTEM image is shown in Fig. 1(d). It can be seen that the atomic sequences are disturbed at the locations of stripes. The $(11\bar{2}0)$ lattice planes are shifted 1/2 interplanar spacing toward $[11\bar{2}0]$, which is characteristic of a stacking fault. Accompanying the periodic shift of the lattice planes, modulated structures are produced. Hence, the modulated structure is caused by a periodic appearance of SFs in the NWs. The periodicity of the modulated structure is about 1.53 nm, which is ten times the $(3\bar{3}00)$ interplanar spacing. In the literature, similar superlattice diffraction patterns were also observed in Fe_2O_3 NWs,[22,23] but no SFs were observed in their HRTEM images. It was thus speculated that the modulated structure was formed by oxygen vacancies. However, we believe that the modulated structure observed in our work is caused by the shear stress along the $[11\bar{2}0]$ direction, which results in the appearance of the SFs. Different growth conditions might lead to the formation of two different modulated structures in Fe_2O_3 NWs.

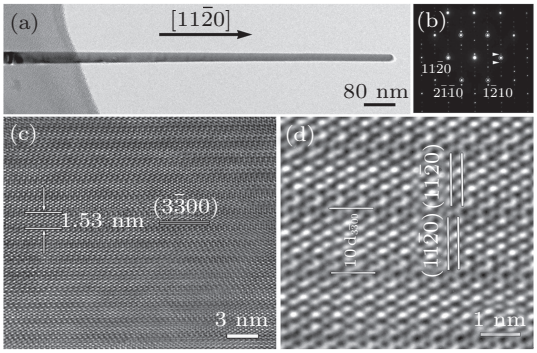

Fig. 1. (a) BF TEM image of a single-crystalline Fe_2O_3 NW; (b) and (c) SAED pattern and HRTEM image for the NW in panel (a), respectively; (d) Enlarged HRTEM image of panel (c).

To confirm that the modulated structure is caused by the SFs instead of oxygen vacancies, EELS spectra have been acquired from an individual Fe_2O_3 NW. Figure 2(a) is the spectrum from a single-crystalline NW with SFs, and figure 2(b) shows the spectra from a single α-Fe_2O_3 NW with oxygen vacancies and pure α–Fe_2O_3 powder. The peaks of the O–K edge at ∼ 532 eV can easily be found in the spectra. In general, peak *a* is derived from the O 1s to 2p core level hybridized with the Fe 3d orbital, while peak *b* originates from the O 2p states hybridized with the Fe 4s and 4p states.[24] Compared with the pure α-Fe_2O_3 powder, Chueh *et al.* thought that the decreased intensity in peaks *a* and *b* is caused by oxygen vacancies inside α-Fe_2O_3 NWs, resulting in a diminishing hybridization of metal 3d orbitals with O 2p orbitals.[22] However, in our spectrum, no evident decrease of the peak intensity can be found in peaks *a* and *b* compared with the α-Fe_2O_3 powder. Therefore, it can be deduced that the modulated structure in our single-crystalline NWs results from SFs instead of oxygen vacancies.

To further investigate the nature of the modulated structure and confirm our experimental results, we constructed an atomic model for the Fe_2O_3 structure and carried out a systematic HRTEM image simulation by changing the thickness and defocus value. Figure 3(a) is the [0001] zone–axis atomic model for the Fe_2O_3 structure. Based on our HRTEM images shown in Fig. 1, the SFs in the Fe_2O_3 NW are produced by shifting 1/2 interplanar spacing of the $(11\bar{2}0)$ planes for every ten $(3\bar{3}00)$ planes. To validate our atomic model, a series of HRTEM images were simulated using a multislice method.

Figures 3(b)–3(i) are the simulated HRTEM images with the same defocus value of 60 nm but with different thicknesses. In these figures, the modulated structure is obvious, which is consistent with the HRTEM image shown in Fig. 1(d). The simulated modulation is also composed of ten $(3\bar{3}00)$ planes and the $(11\bar{2}0)$ planes also have a shift of 1/2 interplanar spacing. It can be deduced that the thickness variation from 24.5 nm to 58.8 nm has no significant effect on the appearance of the modulated structure in the Fe_2O_3NW. Through careful examinations of these images, it can be seen

that when Fe_2O_3 is thin, such as 24.5 nm shown in Fig. 3(b), O atoms (grey) and Fe atoms (white) can be distinguished in the simulated HRTEM image. However, with the increase in the thickness, the contrast for O atoms becomes darker. Eventually, only the white dots that represent the Fe atoms are visible. In addition, it can be also observed that the contrast for white dots becomes increasingly sharp with increasing thickness. However, when the thickness reaches 39.2 nm, the white dots gradually become obscure and at last lose sharp contrast.

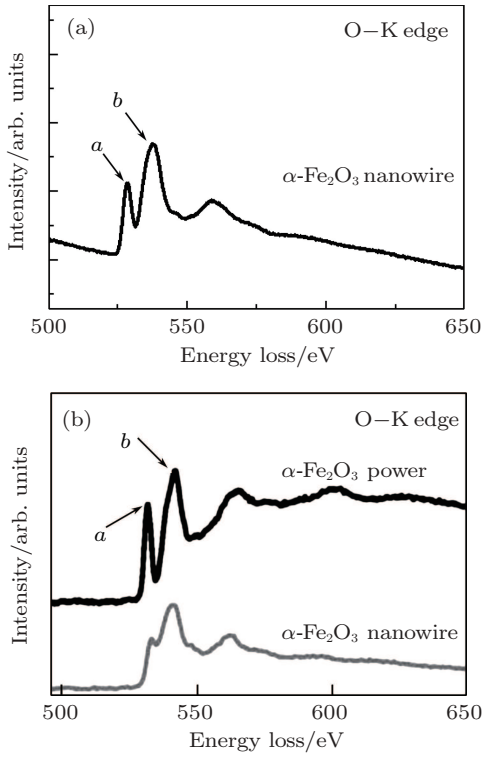

Fig. 2. EELS spectra of (a) a single-crystalline α-Fe_2O_3 NW with SFs; (b) α-Fe_2O_3 NW with oxygen vacancies and α-Fe_2O_3 powder.[22] (Reprinted with copyright permission from Wiley-VCH).

We next look at the defocus effect on the HRTEM image contrast. Figure 4(a) is still the [0001] zone–axis atomic model for the Fe_2O_3 structure. Figures 4(b)–4(i) are simulated HRTEM images with the same thickness (24.5 nm) but with different defocus values. The thickness of Fe_2O_3 is set to be 24.5 nm because it is approximately the same as the experimentally determined diameter of the Fe_2O_3 NW as shown in Fig. 1(a). It can be seen that the simulated modulation is also obvious and is consistent with our HRTEM images. Through careful comparison of these figures, it is obvious that when the defocus value of Fe_2O_3 is not very large, such as 50 nm, the white dots representing the Fe atoms show sharp contrast. However, with the increase of the defocus value, the contrast of these images is reversed such that the white dots become black dots. But this reversal does not lead to the disappearance of the modulated structure.

From the HRTEM simulations, it can be found that the simulated HRTEM image with a thickness of 24.5 nm and a defocus value of 55 nm agrees well with our experimental results. It can be deduced that the simulated images can truly

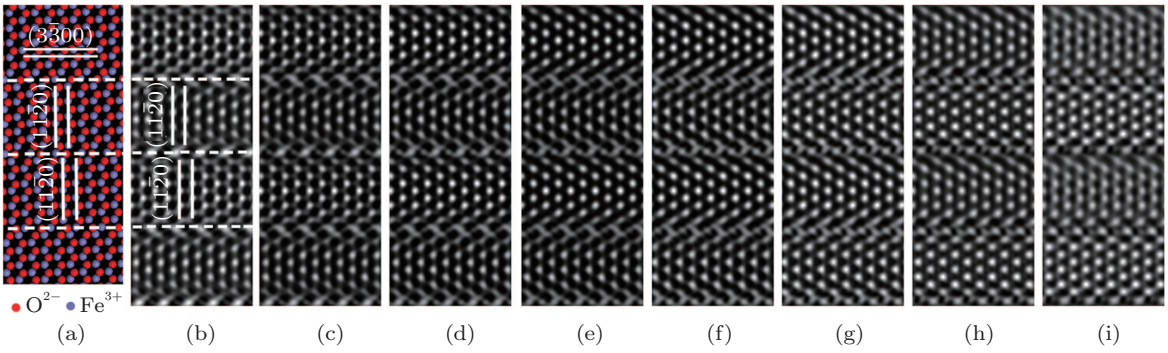

Fig. 3. (color online) (a) [0001] zone–axis atomic model for Fe_2O_3; Simulated HRTEM images with same defocus value of 60 nm but with different thicknesses, (b) 24.5 nm, (c) 29.4 nm, (d) 34.3 nm, (e) 39.2 nm, (f) 44.1 nm, (g) 49 nm, (h) 53.9 nm, and (i) 58.8 nm.

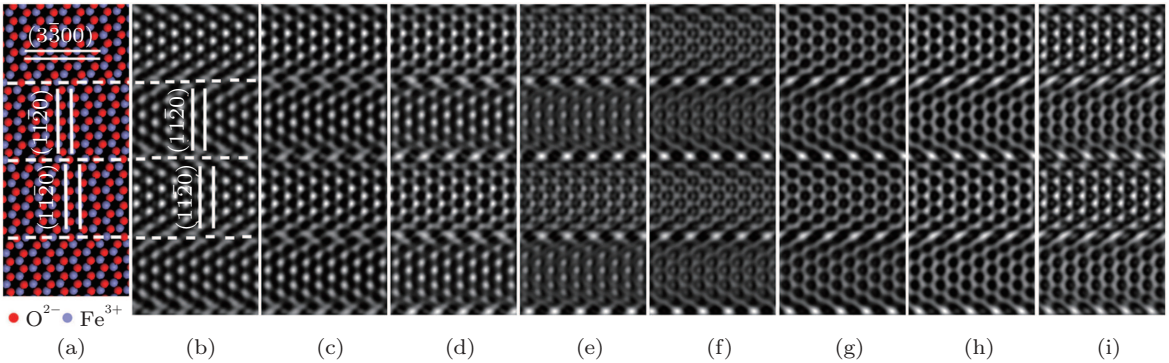

Fig. 4. (color online) (a) [0001] zone–axis atomic model for Fe_2O_3; Simulated HRTEM images for 24.5-nm-thick Fe_2O_3 at different defocus values, (b) 50 nm, (c) 55 nm, (d) 60 nm, (e) 65 nm, (f) 70 nm, (g) 75 nm, (h) 80 nm, and (i) 85 nm.

reflect the essence of this modulated structure. The modulated structure in Fe_2O_3 NWs is caused by the formation of SFs with the $(11\bar{2}0)$ planes shifting 1/2 interplanar spacing for every ten $(3\bar{3}00)$ planes.

4. Conclusion

In conclusion, a new modulated structure has been observed in Fe_2O_3 NWs. The modulated structure is formed by SFs with the $(11\bar{2}0)$ planes shifting 1/2 interplanar spacing over every ten $(3\bar{3}00)$ planes. The periodicity of the modulated structure is 1.53 nm which is ten times the $(3\bar{3}00)$ interplanar spacing. The good match between the simulated and experimental HRTEM images supports our proposed atomic model.

References

[1] Dieckmann R 1993 *Philos. Mag. A* **68** 725
[2] Wang C, Wang F F, Fu X Q, Zhang E D and Xu Z 2011 *Chin. Phys. B* **20** 050701
[3] Chen J, Xu L N, Li W Y and Gou X L 2005 *Adv. Mater.* **17** 582
[4] Tepper T, llievski F, Ross C A, Zaman T R, Ram R J, Sung S Y and Stadler B J H 2003 *J. Appl. Phys.* **93** 6948
[5] Srivastava H, Tiwari P, Srivastava A K and Nandedkar R V 2007 *J. Appl. Phys.* **102** 054303
[6] Shimojo M, Takeguchi M and Furuya K 2006 *Nanotechnology* **17** 3637
[7] Chen Z Q, Cvelbar U, Mozetic M, He J Q and Sunkara M K 2008 *Chem. Mater.* **20** 3224
[8] Cvelbar U, Chen Z Q, Sunkara M K and Mozetic M 2009 *Small* **4** 1610
[9] Nasibulin A G, Rackauskas S, Jiang H, Tian Y, Mudimela P R, Shandakov S D, Nasibulina L I, Sainio J and Kauppinen E I 2009 *Nano Res.* **2** 373
[10] Wang R M, Chen Y F, Fu Y Y, Zhang H and Kisielowski C 2005 *J. Phys. Chem. B* **109** 12245
[11] Wen X G, Wang S H, Ding Y, Wang Z L and Yang S H 2004 *J. Phys. Chem. B* **109** 215
[12] Dong Z, Kashkarov P and Zhang H 2010 *Nanoscale* **2** 524
[13] Fu Y Y, Chen J and Zhang H 2001 *Chem. Phys. Lett.* **350** 491
[14] Yuan L, Wang Y Q, Cai R S, Jiang Q K, Wang J B, Li B Q, Sharma A and Zhou G W 2012 *Mater. Sci. Eng. B* **177** 327
[15] Wang B and Xu P 2009 *Chin. Phys. B* **18** 324
[16] Qin L X, Xue C S, Zhuang H Z, Yang Z Z, Chen J H and Li H 2008 *Chin. Phys. B* **17** 2180
[17] Cai R S, Li T, Wang Y Q, Wang C, Yuan L and Zhou G W 2012 *J. Nanopart. Res.* **14** 1073
[18] Björk M T, Ohlsson B J, Sass T, Persson A I, Thelander C, Magnusson M H, Deppert K, Wallenberg L R and Samuelson L 2002 *Nano Lett.* **2** 87
[19] Gudiksen M S, Lauhon L J, Wang J F, Smith D C and Lieber C M 2002 *Nature* **415** 617
[20] Jiang Y, Meng X M, Liu J, Hong Z R, Lee C S and Lee S T 2003 *Adv. Mater.* **15** 1195
[21] Wang Y Q, Philipose U, Ruda H and Kavanagh K L 2006 *J. Mater. Sci.: Mater. Electron.* **17** 1065
[22] Chueh Y L, Lai M W, Liang J Q, Chou L J and Wang Z L 2006 *Adv. Funct. Mater.* **16** 2243
[23] Lee Y C, Chueh Y L, Hsieh C H, Chang M T, Chou L J, Wang Z L, Lan Y W, Chen C D, Kurata H and Isoda S 2007 *Small* **3** 1356
[24] Colliex C, Manoubi T and Ortiz C 1991 *Phys. Rev. B* **44** 11402